IEEE Access
Multidisciplinary | Rapid Review | Open Access Journal

Received May 24, 2021, accepted June 8, 2021, date of publication June 11, 2021, date of current version June 23, 2021.

Digital Object Identifier 10.1109/ACCESS.2021.3088746

Image Reconstruction Based on Total Variation Minimization for Radioactive Wastes Tomographic Gamma Scanning From Sparse Projections

RUI SHI[1], HONGLONG ZHENG[2], XIANGUO TUO[3], CHANGMING WANG[4], JIANBO YANG[4], YI CHENG[4], MINGZHE LIU[4], AND SONGBAI ZHANG[3]

[1]School of Computer Science and Engineering, Sichuan University of Science and Engineering, Zigong 643000, China
[2]Nuclear Power Institute of China, Chengdu 610005, China
[3]School of Automation and Information Engineering, Sichuan University of Science and Engineering, Zigong 643000, China
[4]College of Nuclear Technology and Automation Engineering, Chengdu University of Technology, Chengdu 610059, China

Corresponding authors: Rui Shi (shirui@suse.edu.cn) and Xianguo Tuo (tuoxg@cdut.edu.cn)

This work was supported in part by the National Natural Science Foundation of China under Grant 41874213, Grant 42074218, and Grant U19A2086; in part by the Key Research and Development Projects in Sichuan Province under Grant 2021YJ0328 and Grant 2021YFSY0058; in part by the Opening Project of Key Laboratory of Higher Education of Sichuan Province for Enterprise Informationalization and Internet of Things under Grant 2019WZJ01; and in part by the Plan Project of Key Technology of Zigong City under Grant 2020YGJC05.

ABSTRACT Tomographic Gamma Scanning (TGS) is one of the most important non-destructive analyzed techniques for radioactive waste drums. By reconstructing the radioactivity distribution image, it can accurately realize the qualitative, quantitative, and positioning analysis of the radionuclides in the drum. However, the time consuming of the scanning is long and the reconstructed image is rough, which limits its good application in the practical assay of the waste drum. In this work, the total variational minimization (TVM) method was applied to improve the iterative process of the conventional algorithms of maximum likelihood expectation maximization (MLEM) and algebraic reconstruction technique (ART), then the MLEM-TVM and ART-TVM reconstruction methods were developed. The transmitted experiments were carried out where four kinds of materials were arranged in a segment whose densities ranging from 1.04 g/cm^3 to 2.02 g/cm^3 and a ^{152}Eu isotope was set up as a transmission source. Compared with the traditional algorithms MLEM and ART, the MLEM-TVM and the ART-TVM algorithms have a better performance on the accuracy and the signal-to-noise ratio, and the MLEM-TVM algorithm achieves the best results, which means the quality of the reconstructed image is improved. The accuracy and effectiveness of the TVM method used in the TGS image reconstruction are verified in the work, and moreover, it can save the scanning time and enhance the TGS image resolution through sparse projection sampling.

INDEX TERMS Image reconstruction, radioactive wastes, tomographic gamma scanning, total variation minimization.

I. INTRODUCTION

Nuclear energy is clean energy compared with thermal power generation, but nuclear power plants will produce a large amount of low and intermediate-level solid radioactive waste with a specific concentration of radionuclides less than 4×10^6 Bq/kg and 4×10^{10} Bq/kg, respectively [1]. Radioactive waste is different from ordinary garbage because it contains radionuclides and needs to be packaged in special nuclear waste drums to reduce radiation hazards and protect the environment. Before classifying and disposal of the radioactive waste, the radiation level must be assessed, so the spatial distribution of radionuclides and their radioactivities in the waste drums should be determined [2], [3]. Considering

The associate editor coordinating the review of this manuscript and approving it for publication was Yunjie Yang.

the radioactive hazards of the radioactive waste, gamma-ray-based non-destructive assay (γ-NDA) is a commonly used technique [4], [5]. The γ-NDA for radioactive waste drums including Segmented Gamma Scanning (SGS) and Tomographic Gamma Scanning (TGS) [6], [7]. The SGS process is convenient and efficient, but it is difficult to accurately analyze non-uniform materials [8]. In contrast, the TGS can accurately reconstruct the medium and radioactivity distribution of the non-uniform drum through three-dimension scanning, so it is more advanced than the SGS [9], [10]. The active (transmission) map, that is the medium distribution reflected by the linear attenuation of the medium, is the basis of the attenuation correction for the radioactivity evaluation [11]. Therefore, an image reconstruction algorithm plays an essential role in the TGS.

The image reconstruction methods can be divided into two categories: resolving reconstruction and statistical iterative reconstruction [12]. Resolving reconstruction methods represented by filtered back-projection (FBP) have fast computed speed but bad signal-to-noise properties, and require complete projections which are time-consuming [13]. However, the iterative reconstruction method, such as algebraic reconstruction technique (ART), maximum likelihood expectation maximization (MLEM), shows strong noise suppression performance and is suitable for incompletely sampling by solving the equations set established by projection data [14], [15]. In addition, some intelligent algorithms are applied in image reconstruction [16], but there is no report on the TGS image. Therefore, the iterative algorithm is the most popular in the problem of TGS image reconstruction [17], [18].

In the industry and commercial field, one high pure germanium (HPGe) with high energy resolution is commonly used as a gamma-ray detector in the TGS system which is confronted with problems of long measurement time and low image resolution that limits its applications in practice [19], [20]. To improve the image quality, it is necessary to increase the number of voxel grids per unit area of a segment, which means increasing the number of projections and scanning time. It should be balanced between image resolution enhancement and time reduction. In 2006, Donoho et al [21] proposed the Compressed Sensing (CS) theory, which utilized random sampling to obtain discrete samples of the signal and can reconstruct the original signal perfectly under the condition that the practical sampling rate is much smaller than the Nyquist sampling rate. The CS has been successfully applied in the fields of medical imaging, optical imaging, capacitance chromatography imaging, et al [22], [23]. For a radioactive waste drum with non-uniform distribution of media, the gamma-ray intensity attenuation by approximate-density materials in a small pixel is less different. Therefore, the transmission image of TGS is locally smooth after the finite-difference transformation and it satisfies the sparseness condition of CS law [21]. On the other hand, if the number of projections is much less than the number of the voxel grids, the image reconstruction equations set is underdetermined. The conventional iterative reconstruction algorithms are hard to get high-quality images. L. Rudin, *et al.* [24], [25] proposed the total variation minimization (TVM) method following the CS theory to remove noise and blur in an image but preserving edges. The TVM provided a novel tool for image restoration and de-noise [26]. In a word, among the various CS methods, the total variation minimization (TVM) is one of the frequently-used means to solve the problem of sparse reconstruction [27], [28].

In this work, based on the MLEM and ART algorithms, the TVM is applied to improve the iterative process of reconstructing the TGS image. It is anticipated to save the scanning time by the means of sparse projections and improve the quality of image combining with the advantages of statistical iterative algorithms and the TVM. Finally, TGS transmission detection experiments are carried out, and the validity and accuracy of the methods are verified and discussed.

II. MATERIALS AND METHODS

A. MLEM ALGORITHM

The gamma-ray with energy E passing through a material follows the law of exponential attenuation, that is

$$I(E) = I_0(E) \cdot exp[-u(E)x], \tag{1}$$

where $I_0(E)$ is the initial intensity of gamma-ray, $I(E)$ is the gamma-ray intensity after attenuation by materials, $u(E)$ is the linear attenuation coefficient which is related to the energy, and x is the transmitting length. Therefore, the TGS transmission measurement of nuclear waste drums can be described as:

$$I_i(E) = I_0(E) \cdot exp\left[-\sum_{j=1}^{N} u_j(E)\, x_{ij}\right], \tag{2}$$

where $u_j(E)$ is the linear attenuation coefficient of the j-th voxel, $j \in [1, N]$, x_{ij} is the transmitting track length of the gamma-ray passing through the j-th voxel when the detector at the i-th position, $i \in [1, M]$, and N is the total number of voxels in a segment and M is the total number of detection positions.

If letting

$$V_i(E) = -ln\left[\frac{I_i(E)}{I_0(E)}\right], \tag{3}$$

then

$$V_i(E) = \sum_{j=1}^{N} u_j(E)\, x_{ij}. \tag{4}$$

Therefore, the matrix form of Eq. (2) is expressed as follows:

$$\boldsymbol{X} \cdot \boldsymbol{U} = \boldsymbol{V}, \tag{5}$$

where $\boldsymbol{X}$ is a $M \times N$ system matrix, $\boldsymbol{U} = (u_1, u_2, \ldots, u_{\mathrm{j}}, \ldots, u_N)^{\mathrm{T}}$, $\boldsymbol{V} = (v_1, v_2, \ldots, v_{\mathrm{i}}, \ldots, v_{\mathrm{M}})^{\mathrm{T}}$.

The reconstruction of the TGS transmission image is to solve the $\boldsymbol{U}$ of Eq. (5) when $\boldsymbol{X}$ and $\boldsymbol{V}$ have been known.

MLEM is a statistical iterative method for image reconstruction with maximizing the likelihood function based on the assumption of Poisson noise [29], [30]. The iterative form of the MLEM algorithm is:

$$u_j^{(k+1)} = \frac{u_j^{(k)}}{\sum_i x_{ij}} \sum_i x_{ij} \frac{v_i}{\sum_j x_{ij} u_j^{(k)}}, \tag{6}$$

where k is the iteration number, and $i\epsilon[1, M]$, $j\epsilon[1, N]$.

B. ART ALGORITHM

ART is based on relaxation methods for solving systems of linear equalities or inequalities [31]. The ART algorithm is expressed in:

$$u_j^{(k+1)} = u_j^{(k)} + \lambda \frac{v_i - \sum_{j=1}^{N} x_{ij} u_j^{(k)}}{\sum_{j=1}^{N} x_{ij}^2} x_{ij}, \tag{7}$$

where λ is the relaxation factor, $0 < \lambda < 2$, and it will affect the reconstructed image quality. Generally, the larger the relaxation factor, the faster the convergence, but the greater the image noise.

The iterative process of MLEM and ART algorithms can be described as follows.

Step 1, assuming an initial image, $u_j^{(1)} = 0$.

Step 2, estimating the projections through forward projection measurements, $\hat{v}_i = \sum_{j=1}^{N} x_{ij} u_j^{(k)}$.

Step 3, comparing the calculated projection with the actual projection, $\Delta_i = \frac{v_i}{\hat{v}_i}$ in MLEM, or $\Delta_i = v_i - \hat{v}_i$ in ART.

Step 4, calculating correction value for the j-th pixel, $C_j = \frac{1}{\sum_{i=1}^{N} x_{ij}} \sum_{i=1}^{N} x_{ij} \Delta_i$ in MLEM, or $C_j = \frac{\Delta_i}{\sum_{j=1}^{M} x_{ij}^2} x_{ij}$ in ART.

Step 5, correcting the j-th pixel, $u_j^{(k+1)} = u_j^{(k)} * C_j$ in MLEM or $u_j^{(k+1)} = u_j^{(k)} + \lambda C_j$ in ART.

Step 6, the result of the k-th iteration is used as the initial value for the $k+1$-th iteration, and the process of step 2 $\sim$ step 5 is looped until the specified number of iterations is met.

Only the pixels that γ-rays pass through are iteratively corrected, while the pixels that do not pass γ-rays are not corrected. Therefore, the ART and MLEM algorithms cannot accurately reconstruct when aiming at the problem of underdetermined equations for reconstructing TGS images.

C. MLEM-TVM AND ART-TVM ALGORITHMS

When $\mathbf{U}$ is the linear attenuation coefficient distribution image, and $u_{m,n}$ represents the pixel value of the m-th row and n-th column of the image, and the finite-difference transform is defined in:

$$\nabla(u_{m,n}) = \sqrt{(u_{m,n} - u_{m-1,n})^2 + (u_{m,n} - u_{m,n-1})^2}. \tag{8}$$

For the finite-difference transform image that is the gradient image, the integral of the L_1-norm of which is the total variation (TV) [32]. It is considered as the objective function. The TV of $\mathbf{U}$ can be expressed in:

$$\begin{aligned} \|u_{m,n}\|_{TV} &= \iint \left|\frac{\partial u}{\partial x}\right| + \left|\frac{\partial u}{\partial y}\right| dxdy \approx \sum_{m,n} |\nabla u_{m,n}| \\ &= \sum_{m,n} \sqrt{(u_{m,n} - u_{m-1,n})^2 + (u_{m,n} - u_{m,n-1})^2}. \end{aligned} \tag{9}$$

Taking the non-negative image value as the basic condition of constraint, the reconstructed image is obtained by solving the following objective function:

$$\min_f \|\mathbf{U}\|_{TV}, \quad s.t.\ \mathbf{V} = \mathbf{X}\mathbf{U}, \tag{10}$$

The solution to minimizing the TV is the image value that needs to be reconstructed. The TV gradient formula of image $\mathbf{U}$ is:

$$\begin{aligned} &\frac{\partial \|\mathbf{U}\|_{TV}}{\partial u_{m,n}} \\ &\approx \frac{2u_{m,n} - u_{m-1,n} - u_{m,n-1}}{\sqrt{\varepsilon + (u_{m,n} - u_{m-1,n})^2 + (u_{m,n} - u_{m,n-1})^2}} \\ &\quad - \frac{u_{m,n+1} - u_{m,n}}{\sqrt{\varepsilon + (u_{m,n+1} - u_{m,n})^2 + (u_{m+1,n} - u_{m+1,n-1})^2}} \\ &\quad - \frac{u_{m+1,n} - u_{m.n}}{\sqrt{\varepsilon + (u_{m+1,n} - u_{m,n})^2 + (u_{m+1,n} - u_{m+1,n-1})^2}}, \end{aligned} \tag{11}$$

where the ε is a minimal positive value introduced for avoiding 0 in the denominator, and usually it was taken an experiential value of 10^{-8}.

The gradient descent method was used to solve the Eq (10) that is the total variation minimization (TVM) process, expressed as follows:

(1) The TV gradient of the image is:

$$\vec{G}^{(k)} = \frac{\partial \|\boldsymbol{U}\|_{TV}}{\partial u_{m,n}}|_{\boldsymbol{U}=\boldsymbol{U}_{TVM}^{(k)}}. \tag{12}$$

(2) The direction of TV gradient is:

$$\hat{G}^{(k)} = \frac{\vec{G}^{(k)}}{|\vec{G}^{(k)}|}. \tag{13}$$

(3) The iterative scheme along the direction of TV gradient descent is:

$$\mathbf{U}_{TVM}^{(k+1)} = \mathbf{U}_{TVM}^{(k)} - \alpha d_A(k) \hat{G}^{(k)}, \tag{14}$$

where α is an adjustment factor, $0.1 < \alpha < 0.5$, $d_A(k)$ is the correction factor, and k is the iteration number of the TVM process. When the adjustment factor α is too small, the reconstructed image has serious noise and poor spatial resolution. When the α is too large, the reconstructed image tends to be blurred because it is too smooth and the spatial contrast decreases. The iteration number k will influence

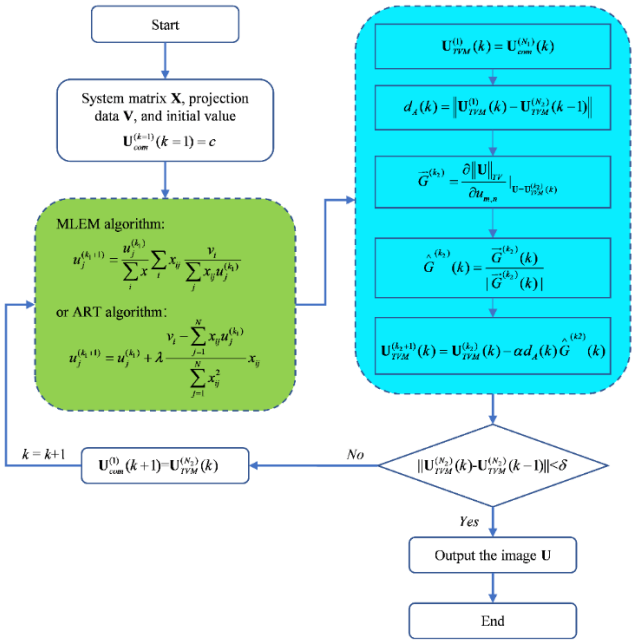

FIGURE 1. Program flow of ART-TVM or MLEM-TVM algorithm, in which δ was set as 10^{-3}.

the reconstructed image quality and the convergence speed. When the k is too small, there are obvious artifacts in the reconstructed image, and as the k increases, the reconstructed image quality is improved, but the convergence is slow.

According to the above algorithms, the transmission image reconstruction of TGS based on TVM iteration was proposed. The program flow is shown in Fig. 1.

Actually, the algorithms can be simply summarized as two steps:

Step 1, ART or MLEM algorithm was adopted to reconstruct an initial TGS image.

Step 2, the TVM process was executed to optimize the quality of the reconstructed image.

III. EXPERIMENTS

The TGS system is developed by ourselves with the following components: a transmission source ^{152}Eu (2.485×10^8 Bq), HPGe gamma-ray spectrometer, collimators of source and detector, a rotating platform of waste drum and controlling system, as Fig. 2 shows. The energy resolution of the HPGe is 1.9 keV @ 1.332 MeV and it is calibrated using a ^{60}Co source. In the present work, one segment samples were designed, and four kinds of waste materials were simulated with different densities: polyethylene (S1) with a density of 1.04 g.cm^{-3}, plastic (S2) with a density of 1.41 g.cm^{-3}, cullet with a density of 1.44 g.cm^{-3} (S3), and concrete (S4) with a density of 2.02 g.cm^{-3}. The size of the TGS system and the random distribution of the materials in the drum are arranged in Fig. 3.

In order to improve the spatial resolution and quality of the image, 12 rings $\times$ 72 angles $=$ 864 grids based on

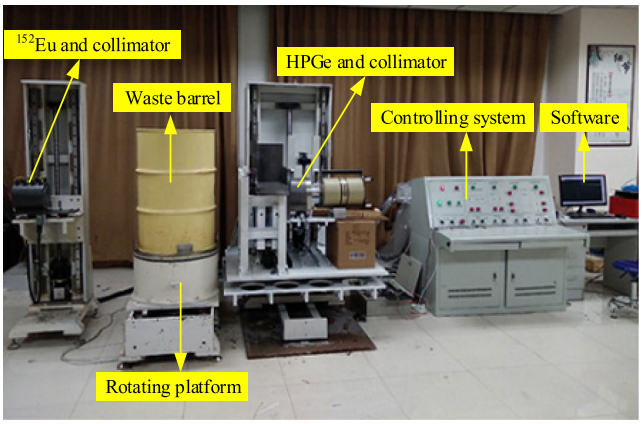

FIGURE 2. TGS system.

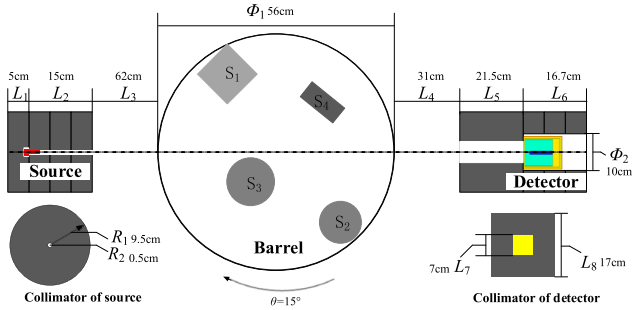

FIGURE 3. Size of the TGS system and the distribution of the materials in the drum.

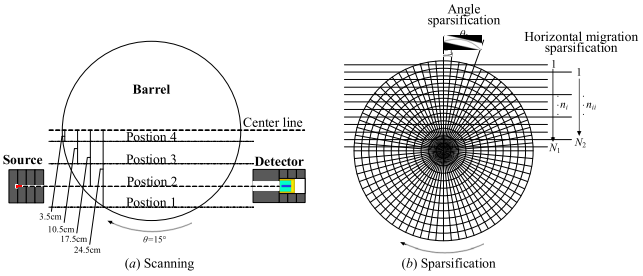

FIGURE 4. TGS transmission scanning process and voxel division model.

polar coordinates were figured to divide the segment shown in Fig. 4b. In the scanning experiments, angle and horizontal sparsifications were applied for reducing the measurement time. Four horizontal positions and 24 rotation positions of the detector were set up as shown in Fig. 4a. 96 transmission gamma spectra were measured by a HPGe detector with 30 seconds per position, so 96 projections were obtained for the segment, that is the measurement time for 96 projections is 1/9 of the 864 grids.

IV. RESULTS AND DISCUSSION

As a way of contrast, the attenuation coefficients of polyethylene, plastic, cullet and concrete were measured using a ^{152}Eu source and its 6 characteristic gamma-ray

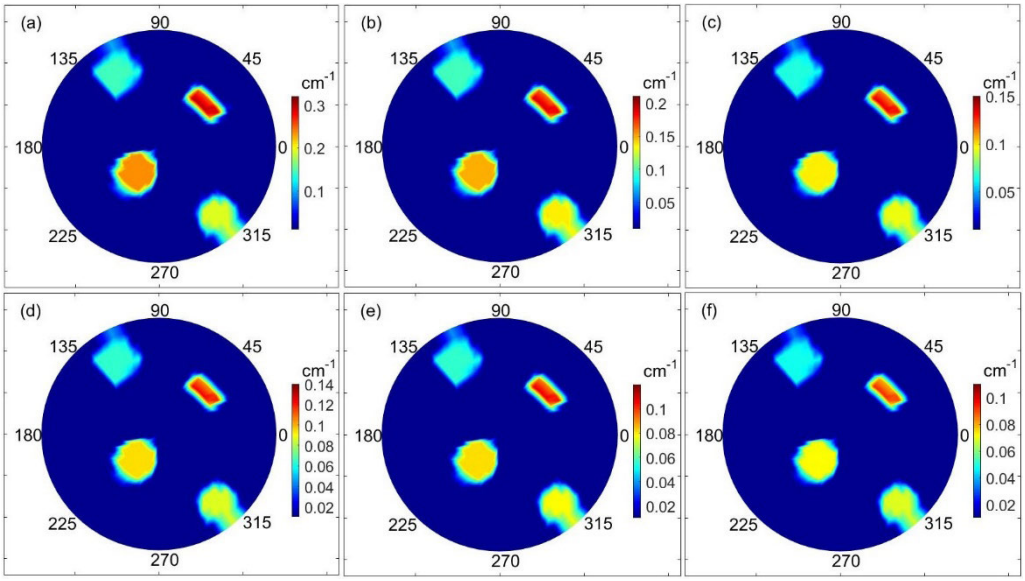

FIGURE 5. Reference images of the transmission.

energies of 0.122 MeV, 0.344 MeV, 0.779 MeV, 0.964 MeV, 1.112 MeV and 1.408MeV were investigated.

The reference images of the transmission with the four materials are shown in Fig. 5, in which the pixel values of the four materials equal in the segment.

As above mentioned, there are 96 projection values for the same gamma-ray energy, but the transmission map has 864 pixels. The equations set are underdetermined in which 864 unknowns must be figured the attenuation coefficients according to the distribution of the materials out from the 96 equations. Therefore, in this work, the TGS image reconstruction is an issue of sparse image reconstruction. For comparison, ART, MLEM, ART-TVM, and MLEM-TVM algorithms were used to solve the equations to reconstruct the TGS image. As a matter of experience, the number of iterations k in MLEM algorithm (Eq. (6)) was set to 20, and the relaxation factor λ in ART algorithm (Eq. (7)) was set to 0.5, and the adjustment factor α in TVM (Eq. (14)) was set to 0.2. The results with 6 energies of ^{152}Eu are shown in Fig. 6, where (a), (b), (c), (d) correspond to the ART, MLEM, ART-TVM, and MLEM-TVM algorithms, respectively. The reconstruction platform was Matlab 2018b on a laptop computer with a processor of i7-CPU.

Apparently from Fig. 6, it can be judged that the images (a) and (b) reconstructed by the ART and MLEM algorithms were rough. The images had serious artifacts and the media shape cannot be distinguished well although the image space resolution was improved. The quality of transmission images (c) and (d) reconstructed by ART-TVM and MLEM-TVM algorithms were significantly better than the images (a) and (b), and the quality of reconstructed images (d) by the MLEM-TVM algorithm was the best relatively and almost free of artifacts. The shape, distribution, and density of the medium in the drum reflected by the image can be well distinguished, and they are consistent with Fig. 3. Aiming at the problem of solving the severely underdetermined equations to reconstruct the transmission image, the iterative algorithm based on the TVM has an obvious optimization effect than the traditional iterative algorithm. The iterative process of TVM makes the artifacts in the area with approximate attenuation converge to the actual distribution, thereby reducing the scattered artifacts. The comparison between (c) and (d) shows that the performance of the MLEM-TVM algorithm is better than that of the ART-TVM algorithm, which illustrated the importance of the initial image that the TVM iteration process relies upon and the initial image quality obtained by the MLEM algorithm is higher than that by the ART algorithm.

In order to objectively judge the pros and cons of different algorithms to reconstruct the TGS image, the mean square error (MSE) and the signal-to-noise ratio (SNR) were utilized to evaluate the reconstructed image. The calculations of MSE and SNR are shown in Eq. (15) and Eq. (16), respectively.

$$MSE = \frac{1}{MN}\sum_{m=1}^{M}\sum_{n=1}^{N}(\mu_{Rec}(m,n) - \mu_{Ref}(m,n))^2 \tag{15}$$

$$SNR = -10\log[\frac{\sum_{m=1}^{M}\sum_{n=1}^{N}(\mu_{Rec}(m,n) - \mu_{Ref}(m,n))^2}{\sum_{m=1}^{M}\sum_{n=1}^{N}(\mu_{Ref}(m,n))^2}] \tag{16}$$

In the formulas, μRec(m, n) and μRef(m, n) respectively represent the reconstructed value and reference value of the m-th row and n-th column of the reconstructed image.

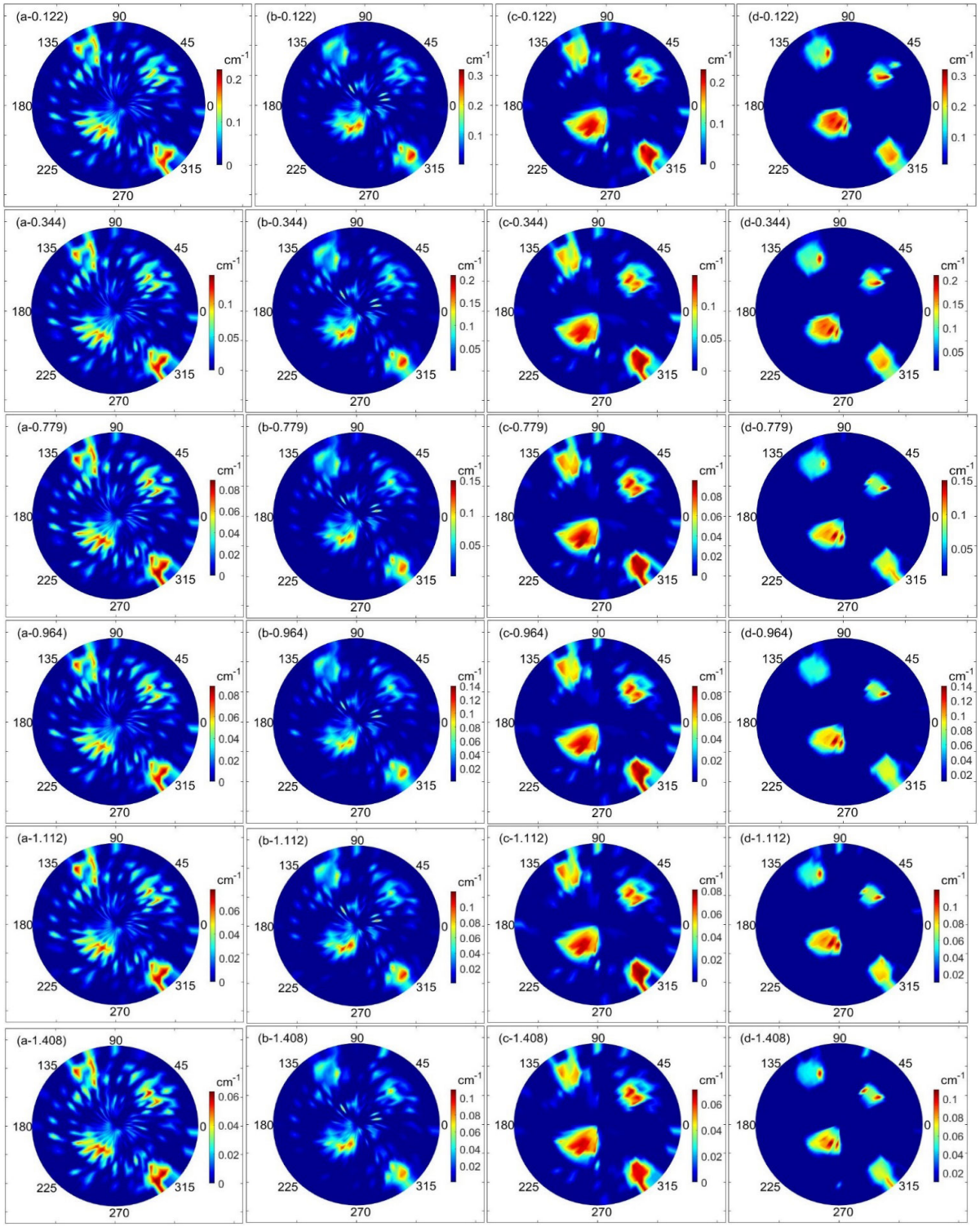

FIGURE 6. Reconstruction images using (a) ART, (b) MLEM, (c) ART-TVM, and (d) MLEM-TVM algorithms with 6 energies.

The MSE and SNR of the TGS transmission images with the above four algorithms are shown in Fig. 7.

The data in Fig. 7 quantitatively verified that compared with the conventional ART and MLEM algorithms the MSE was conspicuously decreased and SNR was increased over 2 times combined with the TVM, and the MLEM-TVM algorithm had the minimum MSE and maximum SNR. For one algorithm, the MSE was decreased with the increase of energy, indicating that the reconstructed values are more accurate with the increase of energy. On the other hand,

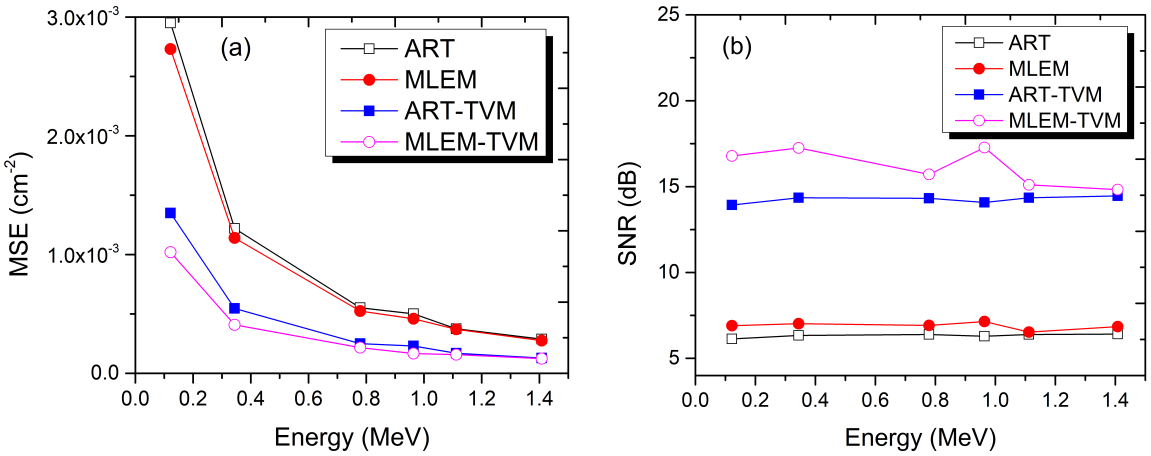

FIGURE 7. (a) MSE and (b) SNR of the TGS transmission images with the ART, MLEM, ART-TVM and MLEM-TVM.

SNR remained relatively stable, and there was no obvious upward or downward trend, which shows that the same image reconstruction method under different energy has little effect on the SNR.

V. CONCLUSION

Non-destructive imaging of low- and medium-level nuclear waste drum is an important means for nuclear waste detection. In this work, combined with the TVM method, the MLEM-TVM and the ART-TVM algorithms were proposed and applied to reconstruct the TGS transmission image. The experimental results show that compared with the traditional iterative algorithm, the MLEM-TVM and the ART-TVM algorithms acquired better outcomes, and the quality of the reconstructed image is higher, and the reconstructed image is more agreed with the actual contents in the drum. Meanwhile, the results reflect the importance of the initial image quality that the TVM iteration process relies on. The image value obtained by the MLEM algorithm is better than the ART algorithm, which makes the MLEM-TVM achieve the best optimization effect.

In summary, utilizing the TVM method have the following advantages than the traditional algorithms:

(1) The artifacts of the reconstructed image are reduced.
(2) The reconstructed values are more accurate.
(3) The SNR of the reconstructed image is enhanced.

Therefore, when solving the underdetermined equations of TGS, the iterative algorithm based on the TVM method has obvious superiority, and the present work verifies the accuracy and effectiveness of the method used for radioactive waste drum samples. Joined the division approach of voxels and sparse projection sampling, the method can effectively improve the TGS image resolution and reduce the measurement time.

ACKNOWLEDGMENT

(Rui Shi and Honglong Zheng contributed equally to this work.)

REFERENCES

[1] D. Beaton, P. Pelletier, and R. R. Goulet, "Microbial degradation of cellulosic material and gas generation: Implications for the management of low- and intermediate-level radioactive waste," *Frontiers Microbiol.*, vol. 10, pp. 1–13, Feb. 2019.

[2] J. Kot'átková, J. Zatloukal, P. Reiterman, and K. Kolář, "Concrete and cement composites used for radioactive waste deposition," *J. Environ. Radioactivity*, vols. 178–179, pp. 147–155, Nov. 2017.

[3] B. Droste, "Packaging, transport, and storage of high-, intermediate-, and low-level radioactive wastes," in *Safe and Secure Transport and Storage of Radioactive Materials*. Sawston, U.K.: Woodhead Publishing, 2015, pp. 231–270.

[4] A. P. Simpson and M. J. Clapham, "International perspective on the application of non-destructive assay technology platforms for sentencing and disposal of radioactive waste-12113," in *Proc. WM Symp.*, Tempe, AZ, USA, Jul. 2012, pp. 1–15.

[5] R. Venkataraman, M. Villani, S. Croft, P. McClay, R. McElroy, S. Kane, W. Mueller, and R. Estep, "An integrated tomographic gamma scanning system for non-destructive assay of radioactive waste," *Nucl. Instrum. Methods Phys. Res. A, Accel. Spectrom. Detect. Assoc. Equip.*, vol. 579, no. 1, pp. 375–379, Aug. 2007.

[6] T. Krings and E. Mauerhofer, "Reconstruction of the activity of point sources for the accurate characterization of nuclear waste drums by segmented gamma scanning," *Appl. Radiat. Isot.*, vol. 69, no. 6, pp. 880–889, Jun. 2011.

[7] T. T. Thanh, H. T. K. Trang, H. D. Chuong, V. H. Nguyen, L. B. Tran, H. D. Tam, and C. V. Tao, "A prototype of radioactive waste drum monitor by non-destructive assays using gamma spectrometry," *Appl. Radiat. Isot.*, vol. 109, pp. 544–546, Mar. 2016.

[8] M. Han, Z. Guo, H. Liu, and Q. Li, "Novel edge treatment method for improving the transmission reconstruction quality in tomographic gamma scanning," *Appl. Radiat. Isot.*, vol. 135, pp. 232–238, May 2018.

[9] R. J. Estep, T. H. Prettyman, and G. A. Sheppard, "Tomographic gamma scanning to assay heterogeneous radioactive waste," *Nucl. Sci. Eng.*, vol. 118, no. 3, pp. 145–152, Nov. 1994.

[10] W. Gu, C. Liu, N. Qian, and D. Wang, "Study on detection simplification of tomographic gamma scanning using dynamic grids applied in the emission reconstruction," *Ann. Nucl. Energy*, vol. 58, pp. 113–123, Aug. 2013.

[11] S. Patra, C. Agarwal, A. Goswami, and M. Gathibandhe, "Attenuation correction for the collimated gamma ray assay of cylindrical samples," *Appl. Radiat. Isot.*, vol. 98, pp. 23–28, Apr. 2015.

[12] X.-Q. Xi, Y. Han, L. Li, and B. Yan, "Tilting fan beam back-projection filtration algorithm for local reconstruction in helical cone-beam computed tomography," *Acta Phys. Sinica*, vol. 68, no. 8, 2019, Art. no. 088701.

[13] S. Li, Z. Dong, Q. Gan, J. Song, and Q. Yang, "An adaptive regularized iterative FBP algorithm with high sharpness for irradiated fuel assembly reconstruction from few projections in FNCT," *Ann. Nucl. Energy*, vol. 145, Sep. 2020, Art. no. 107515.

[14] H. Wieczorek, "The image quality of FBP and MLEM reconstruction," *Phys. Med. Biol.*, vol. 55, no. 11, pp. 3161–3176, May 2010.

[15] S. Li, Z. Dong, Q. Gan, S. Yu, Q. Yang, and J. Song, "A MLEM-TV-MRP algorithm for fast neutron computed tomography reconstruction of high statistical noise and sparse sampling," *IEEE Access*, vol. 8, pp. 3397–3407, Dec. 2020.
[16] L. Cai, P. Luo, G. Zhou, T. Xu, and Z. Chen, "Multiperspective light field reconstruction method via transfer reinforcement learning," *Comput. Intell. Neurosci.*, vol. 2020, pp. 1–14, Jan. 2020.
[17] H. Zheng, X. Tuo, S. Peng, R. Shi, H. Li, A. He, Z. Li, and Q. Han, "An improved algebraic reconstruction technique for reconstructing tomographic gamma scanning image," *Nucl. Instrum. Methods Phys. Res. A, Accel. Spectrom. Detect. Assoc. Equip.*, vol. 906, pp. 77–82, Oct. 2018.
[18] H. Aijing, T. Xianguo, S. Rui, and Z. Honglong, "An improved OSEM iterative reconstruction algorithm for transmission tomographic gamma scanning," *Appl. Radiat. Isot.*, vol. 142, pp. 51–55, Dec. 2018.
[19] T. Roy, M. R. More, J. Ratheesh, and A. Sinha, "Active and passive CT for waste assay using $LaBr_3$ (Ce) detector," *Radiat. Phys. Chem.*, vol. 130, pp. 29–34, Jan. 2017.
[20] T. Roy, M. R. More, J. Ratheesh, and A. Sinha, "A practical fan-beam design and reconstruction algorithm for active and passive computed tomography of radioactive waste barrels," *Nucl. Instrum. Methods Phys. Res. A, Accel. Spectrom. Detect. Assoc. Equip.*, vol. 794, pp. 164–170, Sep. 2015.
[21] D. L. Donoho, "Compressed sensing," *IEEE Trans. Inf. Theory*, vol. 52, no. 4, pp. 1289–1306, Apr. 2006.
[22] J. Zhang, J. Teng, and Y. Bai, "Improving sparse compressed sensing medical CT image reconstruction," *Autom. Control Comput. Sci.*, vol. 53, no. 3, pp. 281–289, Jul. 2019.
[23] J. Provost and F. Lesage, "The application of compressed sensing for photo-acoustic tomography," *IEEE Trans. Med. Imag.*, vol. 28, no. 4, pp. 585–594, Apr. 2009.
[24] L. I. Rudin, S. Osher, and E. Fatemi, "Nonlinear total variation based noise removal algorithms," *Phys. D, Nonlinear Phenomena*, vol. 60, nos. 1–4, pp. 259–268, Nov. 1992.
[25] L. I. Rudin and S. Osher, "Total variation based image restoration with free local constraints," in *Proc. 1st Int. Conf. Image Process.*, 1994, pp. 31–35.
[26] E. J. Candes, J. Romberg, and T. Tao, "Robust uncertainty principles: Exact signal reconstruction from highly incomplete frequency information," *IEEE Trans. Inf. Theory*, vol. 52, no. 2, pp. 489–509, Feb. 2006.
[27] V. Y. Panin, G. L. Zeng, and G. T. Gullberg, "Total variation regulated EM algorithm [SPECT reconstruction]," *IEEE Trans. Nucl. Sci.*, vol. 46, no. 6, pp. 2202–2210, Dec. 1999.
[28] S. J. LaRoque, E. Y. Sidky, and X. Pan, "Accurate image reconstruction from few-view and limited-angle data in diffraction tomography," *J. Opt. Soc. Amer. A, Opt. Image Sci.*, vol. 25, no. 7, pp. 1772–1782, Jul. 2008.
[29] S. Shiba and H. Sagara, "MLEM reconstruction method applied to partial defect verification using simulated data," *Ann. Nucl. Energy*, vol. 139, May 2020, Art. no. 107242.
[30] M. Ravi, A. Sewa, S. T. G., and S. S. S. Sanagapati, "FPGA as a hardware accelerator for computation intensive maximum likelihood expectation maximization medical image reconstruction algorithm," *IEEE Access*, vol. 7, pp. 111727–111735, Aug. 2019.
[31] C. Agarwal, A. Mhatre, S. Patra, S. Chaudhury, and A. Goswami, "Algebraic reconstruction technique combined with Monte Carlo method for weight matrix calculation in gamma ray transmission tomography," *Social Netw. Appl. Sci.*, vol. 1, no. 10, p. 1157, Sep. 2019.
[32] H.-M. Zhang, L.-Y. Wang, B. Yan, L. Li, X.-Q. Xi, and L.-Z. Lu, "Image reconstruction based on total-variation minimization and alternating direction method in linear scan computed tomography," *Chin. Phys. B*, vol. 22, no. 7, Jul. 2013, Art. no. 078701.

RUI SHI received the B.E. degree in nuclear energy and nuclear technology, and the M.E. and Ph.D. degrees in nuclear technology and applications from the Chengdu University of Technology, China, in 2011, 2014, and 2018, respectively. He is currently a Lecturer with the School of Computer Science and Engineering, Sichuan University of Science and Engineering. His research interests include radiation detection, radiation imaging, and nuclear wastes disposal.

HONGLONG ZHENG received the B.E. and M.E. degrees in nuclear energy and nuclear technology from the Southwest University of Science and Technology, in 2013 and 2016, respectively, and the Ph.D. degree in nuclear technology and applications from the China Academy of Engineering Physics, China, in 2019. He is currently an Assistant Researcher with the Nuclear Power Institute of China. His research interests include radiation protection and radiation detection.

XIANGUO TUO received the B.E. degree in radioactive geophysical exploration, the M.E. degree in radioactive geology and exploration, and the Ph.D. degree in nuclear technology and applications from the Chengdu University of Technology, Chengdu, China, in 1988, 1993, and 2001, respectively. From 2006 to 2007, he worked as a Visiting Scholar with the School of Bioscience, University of Nottingham, U.K. Since 2001, he has been a Professor with the College of Nuclear Technology and Automation Engineering, Chengdu University of Technology. Since 2012, he has been a Professor with the School of National Defense Science and Technology, Southwest University of Science and Technology, Mianyang, China. He is currently a Professor in artificial intelligence and robot technology, and the President with the Sichuan University of Science and Engineering, Zigong, China. His current research interests include detection of radiation, nuclear wastes disposal, and specialized robots. He received The National Science Fund for Distinguished Young Scholars, in 2011.

CHANGMING WANG received the B.E. degree in radiation protection and nuclear safety from the University of South China, China, in 2019. He is currently pursuing the degree in nuclear energy and nuclear technology engineering with the Chengdu University of Technology. His research interests include radiation detection, radiation imaging, and nuclear wastes disposal.

JIANBO YANG received the B.E. degree in computer application, the M.E. degree in applied geophysics, and the Ph.D. degree in nuclear technology and applications from the Chengdu University of Technology, China, in 1997, 2008, and 2011, respectively. From 2011 to 2013, he worked as a Postdoctoral Researcher with Tsinghua University, China. Since 2017, he has been a Professor with the College of Nuclear Technology and Automation Engineering, Chengdu University of Technology. His research interests include radiation detection, radiation imaging, and neutron science.

YI CHENG received the B.E. degree in nuclear technology, the M.E. degree in computer application, and the Ph.D. degree in nuclear technology and applications from the Chengdu University of Technology, China, in 1998, 2007, and 2019, respectively. He is currently an Associate Professor with the College of Nuclear Technology and Automation Engineering, Chengdu University of Technology. His research interests include radiation detection, radiation imaging, and specialized robots.

MINGZHE LIU received the B.E. degree in computer application and the M.E. degree in mathematics geology from the Chengdu University of Technology, China, in 1994 and 1997, respectively, and the master's degree (Hons.) and the Ph.D. degree in computer science from Massey University, New Zealand, in 2006 and 2010, respectively. He worked with the Chinese Academy of Engineering Physics, from 1997 to 2004. He is currently a Professor with the College of Nuclear Technology and Automation Engineering, Chengdu University of Technology. His research interests include radiation detection, nuclear medical imaging, and specialized robots.

SONGBAI ZHANG received the B.E. degree in nuclear technology and applications from the University of South China, in 1998, the M.E. degree in particle physics and nuclear physics from Peking University, in 2003, and the Ph.D. degree in particle physics and nuclear physics from the China Academy of Engineering Physics, in 2006. He is currently an Associate Researcher with the School of Automation and Information Engineering, Sichuan University of Science and Engineering. His research interests include radiation detection, radiation imaging, monitoring, and verification technology in nuclear nonproliferation and safeguard.